Role of splicing factor hnRNP-L in cardiac physiology

A thesis submitted by

Wanting Huang

In partial fulfillment of the requirements for the degree of

Master of Science

In

Pharmacology and Drug development

Tufts University

Graduate School of Biomedical Sciences

May 2023

Advisor: Robert Blanton, MD

Abstract

The failing heart demonstrates alterations in gene splicing, suggesting that splicing factors (SFs) may regulate the development of heart failure (HF). However, specific SFs which contribute to this remain unknown. The SF hnRNP-L is a multifunctional RNA-binding protein (RBP) with highly conserved expression in skeletal and cardiac muscle. HnRNP-L is required for normal skeletal myoblast development and function, but its role in the heart has not been investigated. We therefore have investigated hnRNP-L in heart structure and function across species. We observed that hnRNP L protein can be detected in standard blood samples including buffy coat and peripheral blood mononuclear cells from humans and from dogs. In a mouse model of experimental HF, hnRNP-L protein expression increased in left ventricular (LV) tissue from failing hearts, compared with control hearts. To investigate the causal role of hnRNP-L derangements in HF, we bred hnRNP-Lfl/fl mice to transgenic mice expressing αMHC-Cre recombinase, to enable cardiac myocyte-restricted hnRNP-L excision. We observed a approximately 30% reduction of hnRNP-L protein expression in LV tissue from hnRNP-Lfl/+; αMHC-Cre+ mice, compared with hnRNP-Lfl/+; no-Cre littermate controls. We then examined cardiac structure and function by left ventricular echocardiography, invasive LV hemodynamic analysis, and organ masses. We observed no effects of hnRNP-L knockdown on cardiac organ masses or on echocardiographic parameters. However, the hnRNP-Lfl/+; αMHC-Cre+ mice did display reduction in LV developed pressure and in LV relaxation by dP/dt_{min}. These studies represent the first evidence for the role

of hnRNP-L in pathological remodeling in vivo.

Acknowledgments

Words cannot express my gratitude to Blanton's lab, especially Dr.Blanton, for his patience and assistance to my thesis. I have learned a lot from Dr.Blanton about the capabilities that a scientific researcher requires, and it has given me the courage to face the difficulties that I may encounter in scientific research in the future. Also, I want to thank my second reader Dr. Chen for taking the time to provide valuable suggestions for my thesis. I also could not have undertaken this journey without Blanton's lab members, including Gregory L. Martin, Suchita Pande and Loveth Raymond who generously provided technical assistance and expertise. Additionally, this endeavor would not have been possible without the support from Dr.Volchok and Dean's office for their efforts on format editing. I am also grateful to my classmates Lingyun Li and Zhen Li for their suggestions on format.

Lastly, I would be remiss in not mentioning my family, especially my parents. Their belief in me has kept my spirits and motivation high throughout this process. Thanks to my good friends and roommates, Yiwen Ding and Minxin Huang, for supporting me in all respects in my life. I would also like to thank Bubble and Coffee for their mental support.

Finally, I sincerely hope that all the efforts we have made will promote more people in the world to be free from illness and pain. Even my effort is negligible, as the Chinese idiom says, "Constant driving wears away stone", I believe that accumulated efforts can realize all our good wishes.

Table of Contents

List of Tables

List of Figures

List of Abbreviations

αMHC	α-myosin heavy chain
ADBP	Aortic diastolic blood pressure
ASBP	Aortic systolic blood pressure
BW	Body weight
CM	Cardiac myocyte
DBP	Diastolic blood pressure
EDPVR	End-diastolic pressure-volume relationship
EF	Ejection fraction
ESPVR	End-systolic pressure-volume relationship
HF	Heart failure
hnRNP-L	Heterogeneous nuclear ribonucleoprotein L
IVS;d	Intraventricular septal thickness
LA	Left atrium
LV	Left ventricle
LVID;d	Left ventricular internal diastolic dimension
LVID;s	Left ventricular internal systolic dimension
LVPW;d	Left ventricular posterior wall thickness, end-diastolic
PRSW	Preload-recruitable stroke work
RA	Right atrium
RBP	RNA-binding protein
RNP	Ribonucleoprotein
RV	Right ventricle
SBP	Systolic blood pressure
SFs	Splicing factors
TAC	Transvers aortic constriction
TL	Tibia length

Chapter 1: Introduction

1.1 Epidemiology of heart failure

Heart failure (HF) is a syndrome characterized by the reduced ability of heart to pump or fill with blood to meet the metabolic needs of the body[1]. As a global pandemic affecting at least 26 million people world wide, HF prevalence is still increasing and represents the most common cause of cardiovascular death[2]. The prognosis of heart failure is poor, with reported survival estimates of 50% and 10% at 5 and 10 years, respectively, and a marked increase in the risk of sudden death[3]. Currently, HF has no cure, but improved treatments could help patients live a better life with fewer symptoms. Therefore, to further study the mechanism of HF at the molecular level is important and necessary, thus many studies have been conducted to learn about the molecular signaling events in the LV and cardiac myocyte which regulate LV remodeling.

1.2 Gene splicing factors related to heart failure

In most eukaryotic gene expression, precursor mRNA is converted into mature mRNA by splicing. In this process, noncoding sequences (introns) are removed and coding sequences (exons) are ligated together. The complexity of individual genes is enhanced by increasing the number of unique proteins expressed from a single gene. Post-transcriptional modification of mRNA is important for transcription and translation control, which can further promote the diversity of the proteome. Pre-mRNA splicing is catalyzed by spliceosomes, which are multi-megadalton

ribonucleoprotein (RNP) complexes, whose highly dynamic conformation and composition of spliceosomes provide accuracy and flexibility for splicing mechanisms[4]. Multiple splicing factors have been demonstrated to be rich in expression in heart tissue and skeletal muscle, including RNA binding fox-1 homolog 1 (RBFOX1), RNA binding motif protein 20 (RBM20), and RNA binding motif protein 24 (RBM24)[5–7]. Therefore, these findings support a better understanding of the translational significance of dysfunctional specific splicing factors in HF, identifying new therapeutic targets for the disease. However, the specific molecular mechanisms of post-transcriptional modifications of mRNA that regulate pathological cardiac remodeling, remain unknown.

1.3 hnRNP-L study

Therefore, identifying individual SF that regulate left ventricular function and respond to pathological stress may reveal new mechanisms related to cardiomyopathy and potential therapeutic targets for cardiomyopathy. Heterogeneous ribonucleoprotein protein families are trans-acting splicing factors that promote or inhibit splice site recognition. The hnRNPs localize to distinct cellular compartments, undergo post-transcriptional modifications, and affect the metabolism of essential transcripts required by the cell[8].The splicing factor Heterogeneous nuclear ribonucleoprotein L (hnRNP-L) is a multifunctional RNA-binding protein with highly conserved expression in skeletal and cardiac muscle, which is required for normal skeletal myoblast development and function[9,10]. Previous work identified a number of

cardiac-expressed genes with predicted high affinity binding sites for hnRNP L including DMD (Duchenne muscular dystrophy), DTNA (Dystrobrevin Alpha), SLC25A3 (Solute Carrier Family 25 Member 3), TPM1(α-tropomyosin1), TTN(titin), which when mutated lead to cardiomyopathy [11–15]. Among them, it is noted that BIN1(Bridging Integrator 1) also has high affinity binding sites for hnRNP-L, and BIN1 has become a biomarker of heart failure progression and arrhythmia in patients with cardiomyopathy[16]. To conclude, mutations in these genes associate with the development of cardiomyopathy, which suggests the correlation between hnRNP-L and heart diseases. Based on these findings, we hypothesized that hnRNP-L plays a significant role in cardiac development and function through a role in the cardiac myocyte (CM). We also hypothesized that circulating hnRNP-L may serve as a candidate biomarker in HF. To test these hypotheses, we have begun to examine hnRNP-L protein expression in blood samples from mammals, including humans. We have also examined the expression of hnRNP-L in the normal and in the failing left ventricle. Finally, we have investigated the effects of cardiac myocyte-specific knockdown of hnRNP-L on cardiac function and structure in a mouse model.

1.4 Statement of contributions

Wanting Huang wrote the introduction. Dr. Blanton edited and revised the introduction.

Chapter 2: Methods

2.1 Study approval and experimental animals.

Mouse studies were performed in accordance with the Tufts University Institutional Animal Care and Use Committee. Protocol B2021-97. All experimental mice were maintained on a C57BL/6 background (12:12 hour light-dark cycle at 22 ± 2 °C) in the Tufts University Animal Facility.

2.2 Echocardiography

Cardiac echocardiography was performed as described previously[17]. Briefly, mice were anesthetized under 2.5% isoflurane induction, placed on a warming pad under heat lamp, and hair was removed. Anesthesia was reduced to 1.5% and mice equilibrated for at least 7 minutes prior to obtaining images. Images were acquired with a Visualsonics VEVO 2100, in the parasternal long and parasternal short axis.

2.3 Transverse aortic constriction (TAC)

Transverse aortic constriction (TAC) surgery was performed as described as follows[17]. Mice were weighed and then anesthetized with 2.5% isoflurane gas (in 100% oxygen) in the induction chamber. Mice were transferred into a nose cone, maintaining the body temperature at 37 ° C ± 0.5° C by thermal pad and monitored by a rectal thermometer probe. To confirm the mice were at the level of surgical anesthesia due to the absence of toe pinching reflex, anesthesia was maintained at 2.0-2.5% isoflurane (in 100% oxygen). The mice were then injected subcutaneously with

1 mg/kg Buprenorphine SR-LAB (ZooPharm, USA). The left anterior and lateral thorax were shaved, preparing the skin with three povidone iodine/alcohol alternating washes and allowed to dry. Then the area was covered with sterilization drape with an exposing site in the center. We intubated the mice with 22G or 24G angiocatheter, and mechanical ventilation was performed at 80-90 breaths/min with 0.2-0.3ml of ventilation volume (Small Animal Ventilator - Model 687, Harvard Apparatus, USA). A 1cm incision was made in the middle upper chest for blunt dissection of the pectoral and intercostal muscles, and then the ribs were pulled back with a thin retractor. After contraction of the left lung and thymus, determining the transverse aorta and then separated with micro pliers and spring scissors. As quality management, careful dissection of fat and other tissue structures that may change the diameter of the aorta is essential. A 7-0 nylon suture was tied loosely around the aorta transversely (between the carpal artery and the left common carotid artery) with a single knot. Then sterilized blunt-ended 25G, 26G, or 27G needles were placed in the nylon knots alongside the transverse aorta. The knot was completely tightened, including the transverse aorta and blunt end needle, and fixed with a double knot before removing the blunt end needle. The incision was closed by layer suture. Ribs, intercostal muscles, and pectoral muscles were closed with 6-0 absorbable nylon sutures, the skin with 6-0 nylon suture. Removed the mice from the artificial respirator, the tube pulled out and the anesthesia stopped. After lying the sternum, the mice first recovered under the heat lamp and the entire perioperative period was further observed.

Sham surgery was performed the same way but the suture did not remain in place. After 7 days the mice were euthanized and organs harvested as above.

2.4 Pressure Volume-hemodynamic measurements

Mice underwent anesthesia as described above. Next, a Millar pressure and volume-sensing catheter was introduced into the right carotid artery, then into the left ventricle. Pressure and volume measurements were acquired using EMKA software.

2.5 Organ collection.

Mice were deeply anesthetized under 3% isofluorane, hearts were harvested, and then excised into 4 chambers. Organs were rapidly snap frozen in liquid nitrogen, and stored at -80°.

2.6 BCA assay

First, we used the gradient dilution method to create a standard curve of known protein concentration in a 96 well plate. After adding 20 ul of sample to each well, then added 200ul of reagent mixture, incubating the plate at 37 ° C for 30 minutes. Blank was measured on a 540-590 nm spectrophotometer, and we compared the absorbance value with the standard curve to obtain the protein concentration of the sample.

2.7 Tissue preparation and immunoblot

Left ventricular tissue was crushed on dry ice and lysed in TLB supplemented with

1mm PMSF and protease inhibitors (MilliporeSigma, 539134). After clearing the lysates by centrifugation, the protein content was quantified by BCA (Thermo, 23209), and then diluted in 2x Laemmli sample buffer containing SDS (MilliporeSigma, S-3401). Equal amounts of protein from the base of the LV were separated by SDS-PAGE, followed by transfer to nitrocellulose membrane. After blocking in 5% milk/TBST primary antibody to hnRNP-L (Sigma R4903) or to GAPDH in 5% BSA/TBST was applied. Secondary antibody was sheep anti-mouse (Sigma, NA931V). Membranes were visualized using the Protein-Simple FluorChem E system.

2.8 Densitometry.

Blots from the immunoblotting procedure described above were then analyzed to determine the relative abundance of protein on each band. Concentrations were then normalized to a loading control and graphed to compare hnRNP-L protein expression across groups. Densitometry was performed using ImageJ software as described (AJP paper). hnRNP L band density was measured and normalized to GAPDH or to the Ponceau stain. Values are expressed as arbitrary densitometric units.

2.9 Preparation of PBMCs and Buffy Coat.

Blood samples were collected in a specimen tube and mixed by gently inverting for 8-10 s. Tubes were stored upright at room temperature until centrifugation. Immediately prior to centrifugation, tubes were inverted again 8-10 times before centrifuge, then centrifuged at room temperature in a horizontal rotor (swing-out

head) for 20 minutes at 1500 RCF. Approximately half of the plasma was aspirated without disturbing the cell layer. Then, cell layers were collected with a Pasteur pipette and transferred to a 15 ml conical centrifuge tube. PBS was added to bring the volume to 15 ml, then cells were mixed by inverting the tube 5 times. Next, we centrifuged the sample at room temperature for 15 minutes at 300 RCF, aspirating as much supernatant as possible without disturbing cell pellet. The cell pellet was resuspended by gently vortexing or tapping the tube with the index finger, followed by adding PBS to bring the volume to 10 ml. Then the cells were mixed by inverting 5 times. Centrifugation was repeated at room temperature for 10 minutes at 300 RCF and supernatant was aspirated without disturbing cell pellets, leaving enough to be able to resuspend the pellet to be transferred for storage (about 5ml). Samples were stored at -80o.

2.10 Statistical analysis.

Data were analyzed using GraphPad Prism. Data are presented as mean and standard error of the mean. Student's unpaired 2-tailed T test was used to compare two groups. A p value <0.05 was considered statistically significant.

2.11 Statement of contributions

Wanting Huang performed echocardiography and analyzed all experimental data. The animal experiments, including echocardiography, pressure volume-hemodynamic measurements, and TAC surgery were under Gregory L. Martin's help. Wanting Huang performed the echocardiography. The preparation of PBMCs and protocol were

provided by Dr. Kang. The BCA assay and immunoblot were under Suchita Pande's help and suggestion. Figure 3.2 was generated by Timothy Calamaras. All experiments were guided by Dr. Blanton.

Chapter 3: Results

3.1 hnRNP-L protein expression in mammalian blood

To test whether hnRNP-L expression might serve as a readily measurable readout in heart failure, we examined hnRNP-L protein expression in circulating leukocytes from dogs and humans with heart failure (Figure 3. 1). First, we examined hnRNP-L expression in buffy coat from patients with suspected disease-causing mutations of hnRNP-L. We successfully detected hnRNP-L in these samples. Further, the expression of hnRNP-L was higher in proband sample compared to the control group (Figure 3. 1 a,b). We next measured hnRNP-L protein expression in PBMCs isolated from blood samples both of human and of canine patients. We detected no appreciable difference in normalized hnRNP-L expression in PBMCs of the proband compared with control healthy patients (Figure 3. 1 d,e). We found that hnRNP-L protein could be detected in normal dog PBMC samples (Figure 3. 1 c). We concluded that hnRNP-L protein can be detected both in buffy coat fraction and in the PBMC fractions of blood samples in humans and in dogs.

3.2 hnRNP-L protein expression increases in failing left ventricle

Next, to begin to explore the role of hnRNP-L in the cardiac response to pressure overload, a major cause of heart failure, we examined hnRNP-L protein expression in left ventricular tissue from 3-month-old male mice subjected to 7-day transaortic constriction (TAC) or sham surgery. Normalized hnRNP-L protein in LV tissue

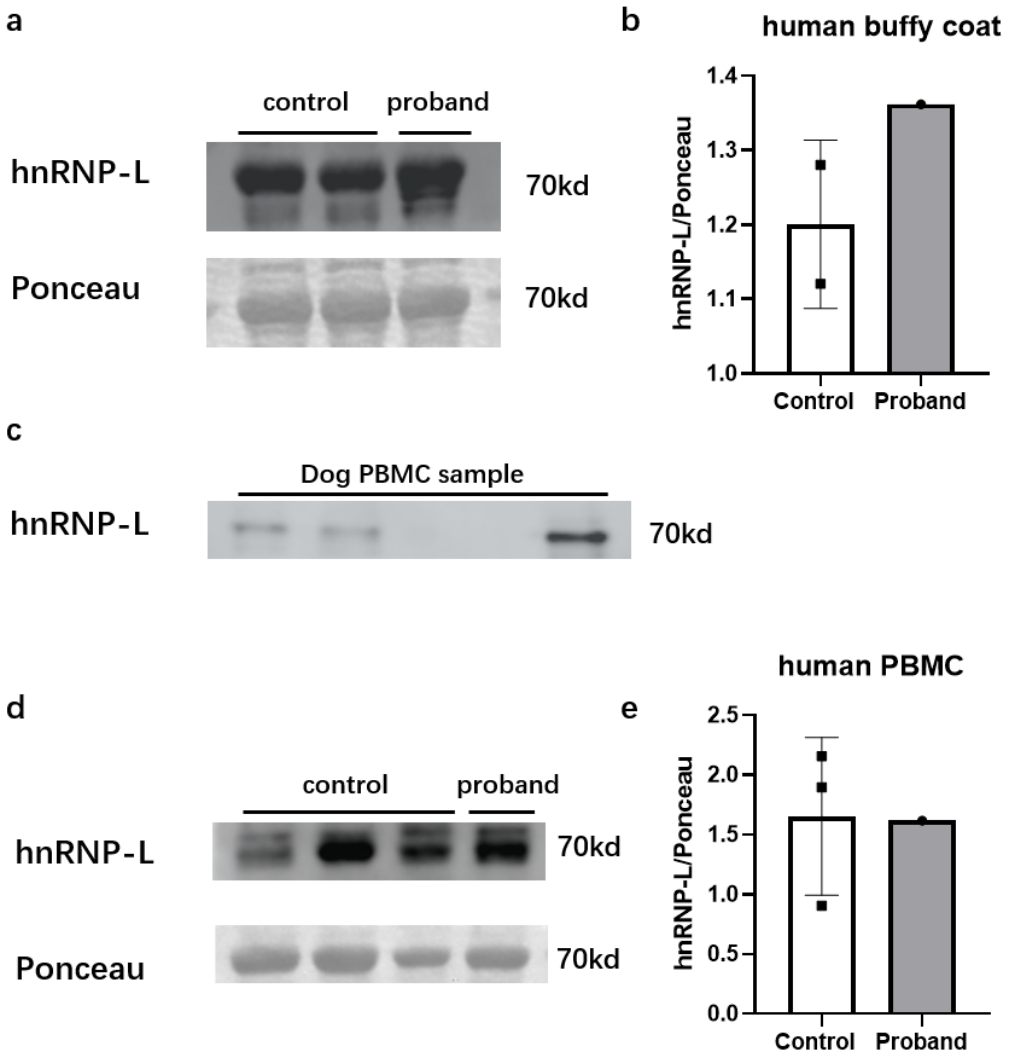

Figure 3. 1 Western blot detection of hnRNP-L in buffy coat and PBMCs from dog and human patients

(A) Representative immunoblot and Ponceau stain, and (B) Quantitation by densitometry, of hnRNP-L in human buffy coat samples. Control denotes healthy human blood sample, and proband denotes human patient with hnRNP-L mutation. (B) Successful detection of hnRNP-L by immunoblot in peripheral blood mononuclear cells (PBMC) isolated from dogs. (C) Representative immunoblot and Ponceau stain, and (D) Quantitation by densitometry, of hnRNP-L in human PBMCs. Control denotes healthy human blood sample, and proband denotes human patient with hnRNP-L mutation.(E)

lysates was increased in TAC group compared to sham group (Figure 3. 2; 0.06 ± 0.01

ADU sham, 0.08 ± 0.02 TAC, $p<0.05$), indicating increased hnRNP-L LV expression

after LV pressure overload.

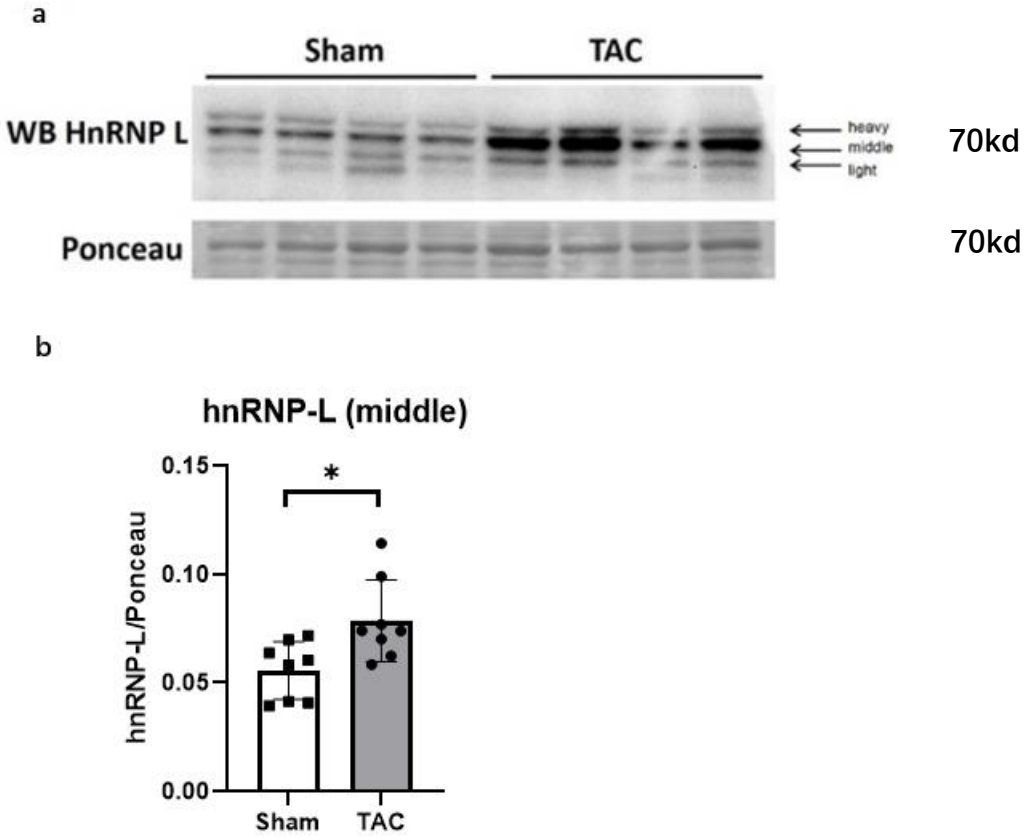

Figure 3. 2 Western blot and quantification of hnRNP-L in left ventricular tissue from Sham and TAC mice.

The expression of hnRNP-L in left ventricle protein lysates was examined by western blot in 3-month-old male mice subjected to 7-day transaortic constriction (TAC) or sham surgery. (A) Representative immunoblot for hnRNP-L, with Ponceau stain as loading control. (B) Quantitation of the middle band of hnRNP-L protein normalized to Ponceau stain. n=8 sham, 8 TAC. *, $p<0.05$ by Student's 2-tailed unpaired T test.

3.3 Effects of hnRNP-L cardiomyocyte-specific knockdown in vivo

The above findings identified that hnRNP-L expression increases in the pressure-overloaded failing LV, supporting its in vivo relevance to LV remodeling. To investigate a potential causative role of hnRNP-L in this process, we examined the effect of cardiac myocyte (CM)-restricted hnRNP-L knockdown on LV structure and function in vivo. To do this, we obtained mice with in which the gene encoding hnRNP-L was flanked by LoxP sites ($hnRNPL^{fl/fl}$), and bred them with a transgenic

mutant strain expressing the Cre recombinase under the control of the alpha myosin heavy chain (αMHC) promotor. We examined the baseline cardiac phenotype of the first generation hnRNP-Lfl/+;αMHC-Cre+ mice to enable cardiac myocyte-restricted hnRNP-L excision.

The expression of hnRNP-L protein in left ventricle was examined by immunoblot. Total normalized hnRNP-L expression appeared reduced in the Cre+ group LVs compared to Cre- (Figure 3. 3 a), indicating Cre-mediated knockdown. Quantitation of hnRNP-L expression normalized to loading control (GAPDH), indicated a significant difference (26.67 % decrease, $p<0.05$) between the hnRNPLfl/+ x αMHC-Cre+ and hnRNPLfl/+ x αMHC-Cre- mice (Figure 3. 3 b).

We then measured the baseline cardiac structure and function by transthoracic echocardiography in hnRNPLfl/+ x αMHC-Cre+ and hnRNPLfl/+ x αMHC-Cre- littermate controls, age 10-12 weeks (Figure 3. 4 and Table 3. 1 Table 3. 2). Echocardiographic analysis of multiple parameters including LV wall thicknesses, diameters, and of LV systolic function (ejection fraction, fractional shortening) revealed no significant changes between the LV structure and function of hnRNPLfl/+ x αMHC-Cre+ mice compared with hnRNPLfl/+ x αMHC-Cre- controls. In sum, hnRNPLfl/+ x αMHC-Cre+ mice did display trends towards pathological structure change in left ventricle, which suggests that the reduced expression of hnRNP-L has certain effect on cardiac function. We also obtained invasive hemodynamic parameters from these mice (Table 3. 1), as a more sensitive measure of LV function.

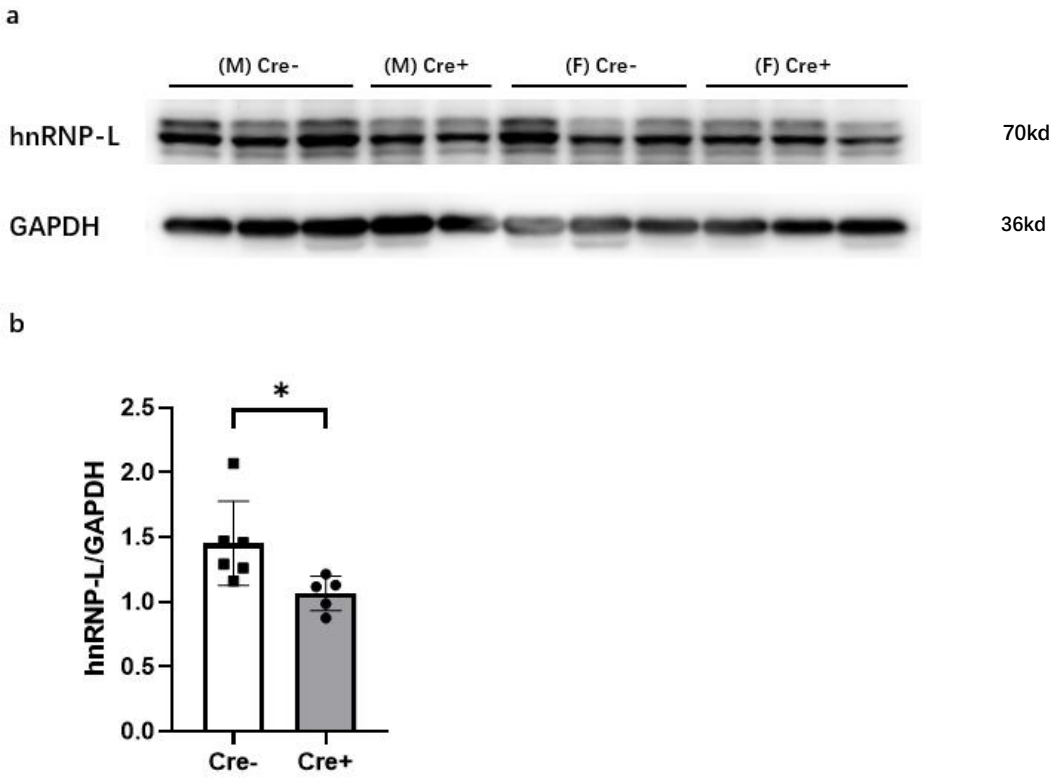

Figure 3. 3 Reduction of hnRNP-L protein expression in LV tissue from hnRNPLfl/+ x αMHC-Cre+ mice.

(A) Representative immunoblot for hnRNP-L or loading control GAPDH, in LV tissue lysates from 3-month-old hnRNP-$L^{fl/+}$ mice with or without transgenic αMHC-Cre expression. (B) Quantitation of normalized hnRNP-L expression by densitometry. n=6 Cre-, 5 Cre+. *, p<0.05 by Student's unpaired 2-tailed T test. Cre- and Cre+ denote absence or presence of αMHC-Cre transgene, respectively.

We detected no significant difference in systolic blood pressure (SBP) and diastolic blood pressure (DBP), but a trend to decline in hnRNPLfl/+ x αMHC-Cre+ mice. Both LV developed pressure and min dP/dt were significantly reduced in Cre+ versus Cre- mice, indicating reduced LV function in the Cre+ mice. Other hemodynamic parameters, however, did not differ significantly between genotypes. We observed no significant differences between the body weights and organ weights in hnRNPLfl/+ x αMHC-Cre+ mice compared with hnRNPLfl/+ x αMHC-Cre-. Specifically, even after

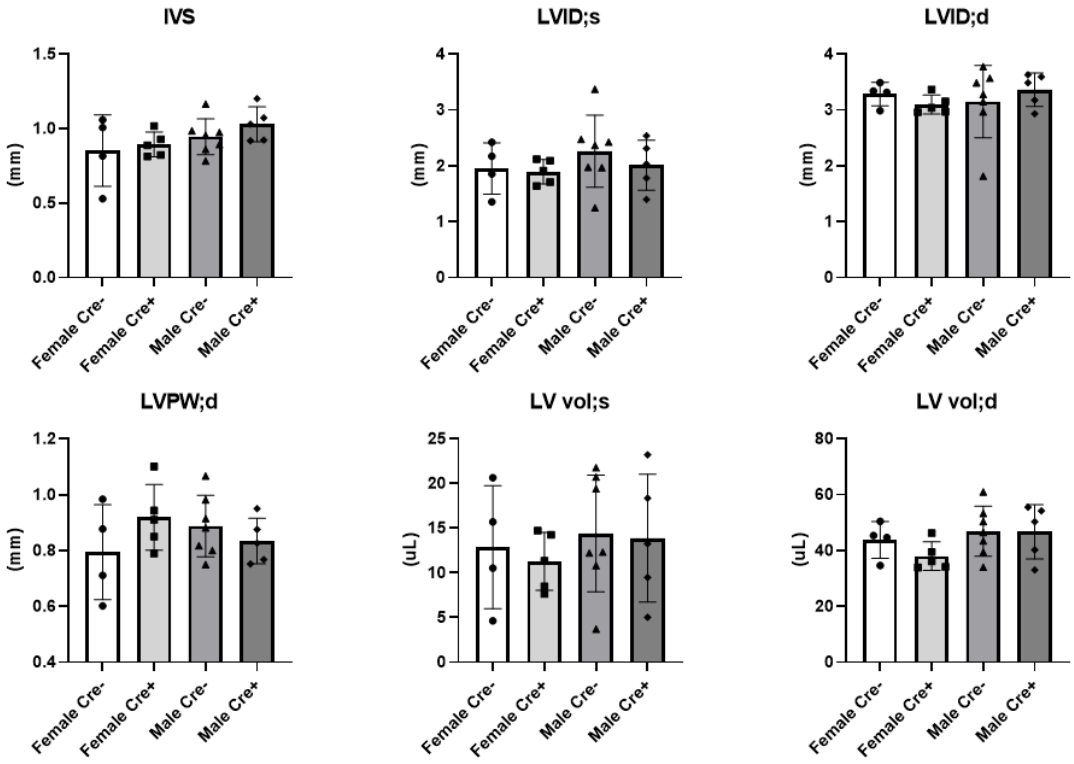

Figure 3. 4 Baseline cardiac structure measured by transthoracic echocardiography in hnRNPLfl/+ x αMHC-Cre+ and hnRNPLfl/+ x αMHC-Cre- mice.

LV, left ventricle; IVSd, intraventricular septal thickness; LVID;s, LV internal systolic dimension; LVID;d, LV internal diastolic dimension; LVPW;d, LV posterior wall thickness; LV vol;d and LV vol;s, LV diastolic and systolic volume, respectively. Groups compared by Student's unpaired 2-tailed T test.

normalized the LV weight to tibia length did not differ significantly (Table 3. 2 and Figure 3. 5). Taken together, these data indicate relatively preserved LV structure in young adult hnRNP-Lfl/fl x αMHC-Cre+ mice, with subtle indications of baseline functional abnormalities at this early age.

3.4 Statement of contributions

Wanting Huang prepared the figures and wrote the chapter. Dr. Blanton provided guidance and edits.

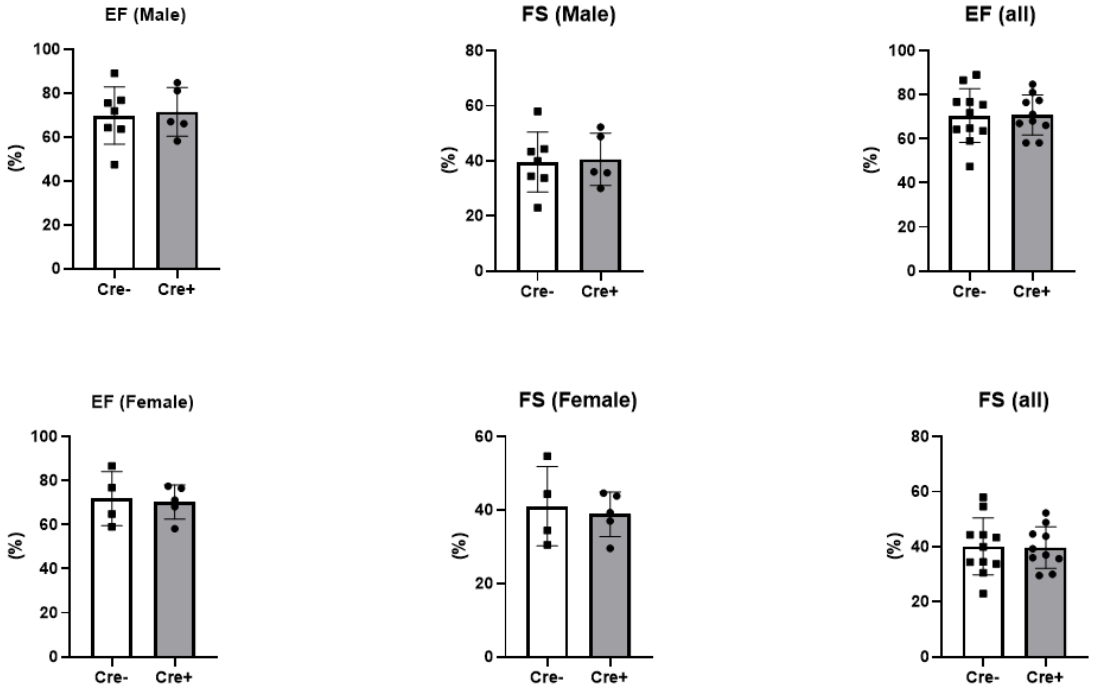

Figure 3. 5 Baseline cardiac systolic function measured by transthoracic.

Echocardiography in hnRNPLfl/+ x αMHC-Cre+ and hnRNPLfl/+ x αMHC-Cre- mice. EF, ejection fraction; FS, fractional shortening. Groups compared by Student's unpaired 2-tailed T test.

	Cre-	Cre+	P value
	n=11	n=10	
A SBP	94.27±8.91	90.1±4.17	0.32
A DBP	63.73±7.5	62.5±5.1	0.72
Maximum pressure, mmHg	92.73±9.9	85.6±4.45	0.07
End diastolic pressure, mmHg	4.73±5.16	4.9±4.18	0.93
Developed pressure, mmHg	93.18±8.45	85.5±4.03	<.05
Relaxation time, msec	38.45±5.07	40.1±2.76	0.44
Max dPdt, mmHg/s	7341.73±770.55	6500.8±1169.29	0.11
Min dPdt, mmHg/s	-6748±786.2	-5599.2±680.2	<.05
Contractility index, 1/s	188.36±18.58	181.2±23.09	0.44
Tau (1/2), msec	5.55±0.85	5.8±1	0.54
Tau (1/e), msec	3.82±0.63	4.2±0.78	0.23
Maximum volume, uL	92.36±16.09	89.7±22.11	0.76
Minimum volume, uL	73.55±10.28	70±14.08	0.53
Stroke volume, uL	19.09±8.8	19.6±11.51	0.91
Cardiac output, uL/min	9210.27±4673.05	9894.2±6021.64	0.78
Ejection fraction, %	19.45±6.93	20.7±9.91	0.75
Effective arterial elastance,mmHg/uL	6.73±3.85	6.3±4.36	0.81
Heart rate, bpm	481.18±61.99	506.6±39.05	0.26
ESPVR, mmHg/uL	4.15±4.44	5.45±4.74	0.51
EDPVR, mmHg/uL	0.26±0.16	0.27±0.11	0.88
PRSW, mmHg*uL	58.8±13.31	62.66±18.54	0.59

Table 3. 1 Left ventricular pressure-volume loop analysis acquired by invasive hemodynamic measurements in hnRNPLfl/+ x αMHC-Cre+ and hnRNPLfl/+ x αMHC-Cre- mice, age 10-12 weeks.

ASBP, aortic systolic blood pressure; ADBP, aortic diastolic blood pressure; ESPVR, left ventricular pressure volume relation; EDPVR, left ventricular diastolic pressure volume relation; PRSW, left ventricular preload-recruitable stroke work. Groups compared by Student’s unpaired 2-tailed t test.

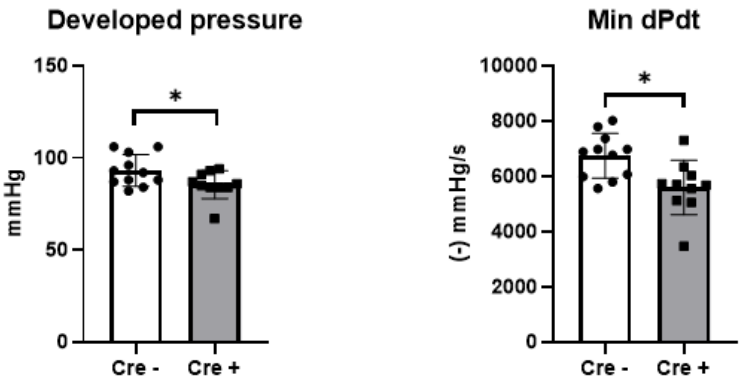

Figure 3. 6 Significant parameters from pressure-volume loop analysis in hnRNPLfl/+ x αMHC-Cre+ and hnRNPLfl/+ x αMHC-Cre- mice, age 10-12 weeks

	Cre-	Cre+	P value
Male	n=7	n=5	
BW, g	26.91±1.52	27±1.22	0.92
LV, mg	94.6±9.17	103.16±6.73	0.11
RV, mg	21±2.24	20.46±1.55	0.65
LA, mg	4±0.98	4.54±1.27	0.42
RA, mg	2.59±0.88	2.48±0.95	0.85
LV/TL, mg/mm	1.55±0.09	1.56±0.06	0.82
RV/TL, mg/mm	0.23±0.06	0.26±0.07	0.41
LA/TL, mg/mm	5.44±0.53	5.96±0.41	0.10
RA/TL, mg/mm	1.21±0.13	1.18±0.09	0.70
Female	n=4	n=5	
BW, g	21.63±2.72	23.2±3.35	0.47
LV, mg	76.38±9.15	76.68±2.39	0.94
RV, mg	15±1.5	16.78±1.59	0.13
LA, mg	2.9±0.59	3.28±0.41	0.29
RA, mg	2.13±0.7	1.86±0.32	0.47
LV/TL, mg/mm	1.28±0.13	1.36±0.18	0.45
RV/TL, mg/mm	0.17±0.03	0.19±0.03	0.27
LA/TL, mg/mm	4.51±0.41	4.51±0.09	0.98
RA/TL, mg/mm	0.89±0.08	0.99±0.08	0.11
All	n=11	n=10	
BW, g	24.99±3.27	24.55±3.27	0.94
LV, mg	87.97±12.65	86.38±13.86	0.75
RV, mg	18.82±3.59	18.4±2.61	0.89
LA, mg	3.6±0.99	3.6±0.59	0.51
RA, mg	2.42±0.82	2.01±0.63	0.48
LV/TL, mg/mm	1.45±0.17	1.46±0.17	0.87
RV/TL, mg/mm	0.21±0.06	0.23±0.06	0.47
LA/TL, mg/mm	5.1±0.66	5.24±0.81	0.69
RA/TL, mg/mm	1.09±0.2	1.08±0.13	0.92

Table 3. 2 Baseline organ masses in hnRNPLfl/+ x αMHC-Cre+ and hnRNPLfl/+ x αMHC-Cre- mice, age 10-12 weeks.

BW, body weight; LV, left ventricle; RV, right ventricle; LA, left atrium; RA, right atrium; TL, tibia length. Groups compared by Student's unpaired 2-tailed T-test.

Chapter 4: Discussion

4.1 Result conclusion

In this study, we examined the role of hnRNP-L in heart failure. We have observed, 1) hnRNP protein is detectable in mammalian blood samples; 2) hnRNP-L expression increases in the failing mouse left ventricle; and 3) genetic cardiomyocyte-specific knockdown of hnRNP-L has no gross effect on cardiac structure in young adult mice, but leads to impaired LV function and relaxation. We conclude from these findings that hnRNP-L likely plays an important role in heart function, especially left ventricle. It is known that hnRNP-L protein is circulating and has already been examined in circulating leukocytes, but it has never been tested in the same type of samples routinely used for patients with heart failure. It remains uncertain whether hnRNP-L expression might serve as a good measurable marker in heart failure patients. In the next stage, it is necessary to ensure the accuracy and sensitivity of this indicator and whether there is a reasonable range to provide early detection of patients. For the human mutant patient, there is a possibility that the inborn mutations in hnRNP-L may cause pathology by changing the expression of the mature protein. Further, we observed possible alternative hnRNP-L isoform in the western blot results, between 37kd-25kd. Future investigation may focus on pathological hnRNP-L subcellular localization, expression, and post-transcriptional processing.

A second important finding of our study is that hnRNP-L protein expression increases in the pressure-overloaded LV. Several possibilities may explain this finding. First, pressure overload may increase hnRNP-L mRNA expression, leading to

higher protein in the cardiac myocyte or in other cells of the LV. Alternatively, LV pressure overload may change the metabolism or degradation of hnRNP-L. A related possibility could be that hnRNP-L expression does not change, but its subcellular localization changes, which leads to alterations in detection by immunoblot. Finally, some combination of these explanations may occur. In future studies we will perform PCR and subcellular localization studies to address these questions. We interpret the finding of increased LV expression of hnRNP-L in the failing LV to support a previously unrecognized role of hnRNP-L in the LV remodeling response. However, these correlative findings cannot determine whether hnRNP-L serves as a marker for HF, opposes HF pathogenesis, or promotes pathological remodeling.

To begin to study the potential causative role of hnRNP-L in this process, therefore, we examined the effects of hnRNP-L knockdown using Cre-Lox technology. To ensure cardiomyocyte-restricted Cre expression (and thus CM-restricted hnRNP-L gene excision), we used the cre-transgene under the control of the α-myosin heavy chain (αMHC). This allowed us to test a heart-specific function of hnRNP-L. In our current study, we examined hnRNP-L fl/fl mice crossed with hnRNP-L +/+; αMHC-Cre+ transgenic mice, in order to generate abundant hnRNP-L fl/+; αMHC-Cre+ and hnRNP-L fl/+; αMHC-No-Cre mice. Due to time constraints, we investigated only $hnRNPL^{fl/+}$ x αMHC-Cre+ mice for research at this stage, with an age range of 10-12 weeks. From the western blot result, we confirmed that the cardiomyocyte-specific knockdown of hnRNP-L is significant. We speculate that the relatively modest, 26%, reduction in hnRNP-L protein in the LV tissue lysates reflects the fact that our lysates

contain non-cardiomyocyte cell types which would not be expected to have hnRNP-L deletion. Future studies will examine hnRNP-L expression in isolated CMs.

Our in vivo echocardiographic showed no significant changes in LV structure and function between control and hnRNP-L CM-specific deletion mice. This is probably due to the partial knockdown in LV cardiomyocyte is not as expected. At the same time, due to time limits, the age of mice is not old enough to display more obvious pathological structure change, but only a trend. Similarly, we observed no statistically significant differences in body weights and organ weights between genotypes. We did observe trends towards cardiac chamber hypertrophy in the hnRNPLfl/+ x αMHC-Cre+ mice, suggesting an in vivo effect of hnRNP-L knockdown. With more sensitive hemodynamic parameters, we did observe significant differences in LV developed pressure and min dP/dt. This suggests that knockdown of hnRNP-L in cardiomyocytes impairs LV function. We interpret this to suggest that hnRNP-L may normally oppose LV dysfunction and remodeling through a role in the cardiac myocyte. Future studies will examine the baseline, and the LV pressure overload phenotype of homozygous flox mice which we predict will have a more robust phenotype, if our hypothesis is correct. We also note that it remains a possibility that the reduced LV function in hnRNP-L fl/+; aMHC-Cre+ mice reflects a toxic effect of the Cre protein, rather than a primary effect of hnRNP-L knockdown. This is unlikely, however, because our previous observations do not detect a toxic effect of Cre at the 10-12 week age (Blanton lab, unpublished results). However, future studies will use hnRNP-L +/+ ; aMHC-Cre controls to test this formally.

To conclude, we observed that hnRNP-L plays a role in maintaining left ventricular function and its downregulation changed the heart function slightly in vivo. Future work is needed to validate the hypothesis that hnRNP-Lfl/fl x αMHC-Cre+ mice will display LV dysfunction and more severe cardiac remodeling compared with controls. Also, we speculate about whether hnRNP-L can be observed to have a more obvious protective effect if TAC and sham surgery are performed on hnRNP-Lfl/+ x αMHC-Cre+/- mice, as there is no other additional pressure on the heterozygous mice LV. From the clinical perspective, it is uncertain whether this up-regulation of hnRNP-L occurs as a consequence of pathological structure change, or rather as a compensatory mechanism. If these hypotheses are confirmed, we will explore diagnostic strategies using hnRNP-L in conditions such as HF with preserved LV ejection fraction, and we will explore therapeutic strategies to augment hnRNP-L in HF.

This study has several limitations. First, due to time constraints we did not have the opportunity to examine older hnRNPLfl/+ x αMHC-Cre+ mice. Thus, the effect of hnRNP-L on heart function in aging mice remains unknown. Similarly, we have not yet had the chance to study these mice in the setting of TAC. Second, we did note some trends of hypertrophy are observed in the hnRNPLfl/+ x αMHC-Cre+ mice, so it is possible that our study is statistically underpowered to detect a small degree of cardiac hypertrophy. Finally, as discussed above, the possibility of cardiotoxicity of Cre in cardiomyocyte should be considered.

In conclusion, the study indicated that the hnRNP-L preserved LV structure and function, as reduced expression of hnRNP-L has certain effect on LV. The results also

provide evidence for hnRNP-L serving as a measurable maker in the future.

4.2 Statement of contribution

Wanting Huang wrote the chapter. Discussion writing was guided and revised by Dr. Blanton.

Chapter 5: Bibliography

1. Coronel, R., de Groot, J. R. & van Lieshout, J. J. Defining heart failure. *Cardiovasc. Res.* **50**, 419–422 (2001).
2. Savarese, G. & Lund, L. H. Global Public Health Burden of Heart Failure. *Card. Fail. Rev.* **3**, 7–11 (2017).
3. Cowie, M. R. *et al.* Survival of patients with a new diagnosis of heart failure: a population based study. *Heart Br. Card. Soc.* **83**, 505–510 (2000).
4. Will, C. L. & Lührmann, R. Spliceosome structure and function. *Cold Spring Harb. Perspect. Biol.* **3**, a003707 (2011).
5. Boeckel, J.-N. *et al.* SLM2 Is A Novel Cardiac Splicing Factor Involved in Heart Failure due to Dilated Cardiomyopathy. *Genomics Proteomics Bioinformatics* **20**, 129–146 (2022).
6. Yang, J. *et al.* RBM24 is a major regulator of muscle-specific alternative splicing. *Dev. Cell* **31**, 87–99 (2014).
7. Gao, C. *et al.* RBFox1-mediated RNA splicing regulates cardiac hypertrophy and heart failure. *J. Clin. Invest.* **126**, 195–206 (2016).
8. Martino, F. *et al.* The mechanical regulation of RNA binding protein hnRNPC in the failing heart. *Sci. Transl. Med.* **14**, eabo5715 (2022).
9. Chang, M.-W. *et al.* Enhanced myogenesis through lncFAM-mediated recruitment of HNRNPL to the MYBPC2 promoter. *Nucleic Acids Res.* **50**, 13026–13044 (2022).
10. Song, Y. *et al.* LINC01588 regulates WWP2-mediated cardiomyocyte injury by interacting with HNRNPL. *Environ. Toxicol.* **37**, 1629–1641 (2022).
11. Kamdar, F. & Garry, D. J. Dystrophin-Deficient Cardiomyopathy. *J. Am. Coll. Cardiol.* **67**, 2533–2546 (2016).
12. Cao, Q. *et al.* Phenotype and Functional Analyses in a Transgenic Mouse Model of Left Ventricular Noncompaction Caused by a *DTNA* Mutation. *Int. Heart. J.* **58**, 939–947 (2017).
13. Kwong, J. Q. *et al.* Genetic deletion of the mitochondrial phosphate carrier desensitizes the mitochondrial permeability transition pore and causes cardiomyopathy. *Cell Death Differ.* **21**, 1209–1217 (2014).
14. England, J. *et al.* Tropomyosin 1: Multiple roles in the developing heart and in the formation of congenital heart defects. *J. Mol. Cell. Cardiol.* **106**, 1–13 (2017).
15. Tharp, C. A., Haywood, M. E., Sbaizero, O., Taylor, M. R. G. & Mestroni, L. The Giant Protein Titin's Role in Cardiomyopathy: Genetic, Transcriptional, and Post-translational Modifications of TTN and Their Contribution to Cardiac Disease. *Front. Physiol.* **10**, 1436 (2019).
16. Zhou, K. & Hong, T. Cardiac BIN1 (cBIN1) is a regulator of cardiac contractile function and an emerging biomarker of heart muscle health. *Sci. China Life Sci.* **60**, 257–263 (2017).
17. Richards, D. A. *et al.* Distinct Phenotypes Induced by Three Degrees of Transverse Aortic Constriction in Mice. *Sci. Rep.* **9**, 5844 (2019).